A Hybrid Stability Index and Harris Hawks Optimization for the Optimal Reallocation of Generators in the Presence of SVC

J. Ayyappa[1,2], Dr. N. Jayakumar[3], Dr. A. Srinivasa Reddy[4]

[1]*Research Scholar, Department of Electrical and Electronics Engineering, Annamalai University, Annamalai Nagar, Chidambaram, Tamil Nadu, India*
[2]*Assistant Professor, Department of Electrical and Electronics Engineering, Sir C R Reddy College of Engineering, Eluru, Andhra Pradesh, India*
Email: ayyappacrr@gmail.com
[3]*Assistant Professor, (Deputed from Annamalai University) Lecturer, Dept. of EEE Government Polytechnic College, Ariyalur. Tamil Nadu, India.*
Email: jayakumar_382@yahoo.co. in
[4]*Professor & HOD, EEE Dept., Sir C. R. Reddy College of Engineering, Eluru, India.*

Abstract: Increasing system efficiency and dependability in a very competitive power market depends on best use of available resources. This work offers a hybrid approach for generator tuning and Static VAR Compensator (SVC) placement selection to enhance system performance. The perfect generator settings are found using the Harris Hawks optimization (HHO) method; a hybrid stability index (HSI) is then used to choose the best SVC location. Measuring voltage stability, the HSI combines the Vi/Vo index with the L-index. A multi-objective function is developed to lower losses, lower the cost of power generating, and improve voltage stability. The proposed method was tested on an IEEE 30-bus system under both normal operating settings and extreme system disturbances brought on by line outages. Under both normal and fault situations, the results show the effectiveness of the HHO-based approach in raising power system stability and operational performance when compared to those obtained using the Harmony Search (HS) technique.

Keywords: Hybrid Stability Index (HSI), Harris hawks optimization (HHO), Static VAR Compensator (SVC), Generator Tuning, Power System Optimization, Voltage Stability, Multi-Objective Function, L-index, Vi/Vo Index, IEEE 30-Bus System, Contingency Analysis, Flexible AC Transmission System (FACTS).

1. Introduction

The sector on electrical power has become a more demanding and competitive one. Secure, effective, and steady working of power systems is ever more needed in modern commercial and technical advances. Rising load demands, the emergence of deregulated electrical markets, integrating renewable energy sources, and other factors push utility providers more and more to keep optimal performance. Controlling the resource allocation processes, optimal maintenance of voltage profiles, achieving minimum loss of active power, and preserving overall system stability present other difficulties. Coordinated application of FACTS devices, sophisticated optimization techniques, and comprehensive contingency analysis frameworks [1–3] allows one to reach these challenging goals.

Particularly SVCs, STATCOMs, and UPFCs, the devices FACTS have become very effective tools to improve the controllability and capacity growth in the transmission of power systems [4–6]. Improving voltage control depends on shunt linked SVCs since they improve system dependability and voltage stability. For a more "compelling" case, their placement is often guided by metrics of voltage stability like L index, Fast Voltage Stability Index FVSI, Voltage Sensitivity Index VSI, etc., which can detect

the most compensable buses and are considered point focus for damage mitigating in the network [7–9]. The devices need to be ideally placed in the system.

Reallocation of generators is another crucial optimization activity in planning and operation of the power system. Allocation of generation among the given units guarantees economical operation, increases voltage support, preserves system frequency, and improves power flow distribution [10–12]. In some circumstances, improperly distributed generators could cause voltage declines and higher losses; in other cases, under stressed or contingency conditions, they could cause severe system instability. System load, system topology, and reactive power demand all help to guide generator output allocation thereby preserving equilibrium in the power system. In contingency scenarios, where changes of generation can prevent a cascading failure and support voltage stability across the interconnections, it becomes essentially more crucial. Therefore, combining generation reallocation with FACTS allocation integrated inside the optimization design provides a better view of the general system dependability and efficiency [13–15].

Recent metaheuristic algorithms are most usually utilized in place of conventional optimization techniques to control the complex and highly non-linear problem of power system optimization. Natural and biological events guide Genetic Algorithm (GA), Particle Swarm Optimization (PSO), Ant Lion Optimizer (ALO), Krill Herd (KH), Harmony Search (HS), and Harris Hawks Optimization (HHO) into flexible and successful search strategies [16–19]. Of these, HHO has been of attention since it can balance exploration and exploitation suitably, hence suitable for addressing non-convex optimization problems including optimal power flow (OPF) and voltage stability augmentation. In the framework of power systems, empirical investigations have shown that HHO achieves better than most conventional approaches in the rate of convergence, robustness, and the quality of the solution [20–22].

Modern power systems require multi-objective optimization since several operational goals have contradicting character. These goals are minimizing total active power losses, voltage variation, fuel generation cost, and system voltage stability margins. Using a weighted sum approach, a standard multi-objective function used in OPF combines various objectives under which the whole objective function is computed as a sum of generation cost, power losses, voltage variation, and stability index, weighted by their respective weights. Thus, one guarantees the balanced trade-off between technical performance and economic optimality [23–25].

Evaluating power system security and resilience against unanticipated transmission line or generator outages depends critically on contingent analysis. Popular N-1 contingency studies if the system can sustain single-component failures without exceeding operating constraints [26–28]. Indices include the L-index, Vi/Vo ratio, and composite measures like the HSI help one to evaluate the degree of each contingency. These indices help to identify the most severe contingency and enable the planning of remedial actions, such as appropriate positioning of FACTS devices and generator re-allocation, to prevent possible instabilities before they show [29].

Using hybrid approaches combining intelligent optimization algorithms with voltage stability and contingency analysis tools is one of the developing trends in power system optimization studies. Applying the HHO method and HSI, for example, can offer a more exact and flexible way to adjust generator outputs and best locate SVCs both under faulted and normal operation. These hybrid models provide robust, real-time control methods, react well to system contingencies, and simultaneously solve numerous objectives. Case histories using standard test systems, the IEEE 30-bus network has shown that these integrated approaches perform substantially better than conventional methods both in terms of optimization outcomes and system stability improvements [30].

2. HYBRID STABILITY INDEX PROPOSAL

Using the L-index and Vi/Vo index from equation (1), a Hybrid Stability Index (HSI) is created.

$$HSI = Z_1 \times S_1 + Z_2 \times S_2 \quad (1)$$

Here, Z1 and Z2 are the weighting elements. Z1 and Z2 have values of 0.5 and 0.5, respectively. Equation (2) provides the L-index, denoted S_1.

$$S_1 = \left|1 - \sum_{i=1}^{g} F_{ji} \frac{V_i}{V_j}\right| \quad (2)$$

L-index S_1 assumes a value between 0 and 1. The smaller the value of the index, the higher the system stability. F_{ji}, which is one of the elements in the F-matrix, is Load participation factor. F-matrix is the sub-array of partial inverse for node admittance matrix. F_{ji} depicts these complex elements. V_i indicates

the voltage magnitude at bus i and V_j indicates the voltage magnitude at bus j. Equation (3), where Vi is the reference voltage and Vo is the output voltage, yields the Vi/Vo index, or index S2.

$$S_2 = 1 - \frac{V_i}{V_o} \quad (3)$$

3. PROBLEM FORMULATION:

For the best generator tuning, a multi-objective function that considers the fuel cost, real power loss, and voltage variation was employed.

$$\text{Min } F = \text{ Min } (W1 * F1 + W2 * F2 + W3 * F3) \quad (4)$$

Where, F1 is the Fuel cost given by

$$F1 = \min \left(\sum_{i=1}^{ng} \left(a_i + b_i P_{Gi} + C_i P_{Gi}^2 \right) \right) \quad (5)$$

The number of generators in the power system is represented by Ng and the fuel cost coefficients are a, b, and c. Table.1 lists the values of the coefficients for the several generators.

Table.1: Fuel Cost Calculation Values for a, b, and c

Generator bus no	a (p.u)	b (p.u)	c (p.u)
1	0.005	2.45	105
2	0.005	3.51	44.1
5	0.005	3.89	40.6
8	0.005	3.25	0
11	0.005	3	0
13	0.005	2.45	105

In this case, there are ntl transmission lines and Sjk is the total complex power flowing from bus j to bus k in line i, where F2 denotes the voltage variance.

$$F2=\min (VD)=\min \left(\sum_{k=1}^{Nbus} \left(V_K - S_k^{ref} \right)^2 \right) \quad (6)$$

The reference value of the voltage magnitude at bus is V_k^{ref}, whereas the actual voltage magnitude at bus k is V_k.

The true power loss is F3.

$$F3=\min \left(\sum_{i=1}^{ntl} \text{real}\left(S_{jk}^i + S_{kj}^i \right) \right) \quad (7)$$

Equality constraints:

Power Balance Constraint

$$\sum_{i=1}^{N} P_{Gi} = \sum_{i=1}^{N} P_{Di} + P_L \quad (8)$$

$$\sum_{i=1}^{N} Q_{Gi} = \sum_{i=1}^{N} Q_{Di} + Q_L \quad (9)$$

Where i=1, 2, 3... N and N = no. of. PL indicates the active power loss of the system, Q_L is the total reactive power loss, P_{Gi} is the active power generated at bus i, Q_{Gi} is the reactive power generated at bus i, P_{Di} is the power demand at bus i, Q_{Di} is the power demand at bus i, and N is the number of buses.

Inequality constraints:

Voltage balance constraint

$$V_{Gi}^{\min} \le V_{Gi} \le V_{Gi}^{\max} \quad (10)$$

Where Gi=1, 2, 3... ng and ng = number of Generator buses.

Real power generation limit:

$$P_{Gi}^{\min} \le P_{Gi} \le P_{Gi}^{\max} \quad (11)$$

Where, Gi=1, 2, 3... ng

where ng is the number of generator buses. The voltage limits of the generator buses are taken between 0.9 p.u and 1.1 pu.

Reactive Power generation limits:

$$Q_{Gi}^{\min} \le Q_{Gi} \le Q_{Gi}^{\max} \quad (12)$$

The limitations of the FACTS controllers SVC include the aforementioned disadvantages in deciding generation reallocation and optimum sizing of the device with methods to optimize.
SVC Limit

(13)

$$B_{svc}^{\min} \le B_{svc} \le B_{svc}^{\max}$$

4. PROPOSED APPROACH

This work presents a methodical four-stage power system optimization model that combines the benefits of HHO and HS algorithms. By lowering the generating cost, power losses, and voltage variations, the technique aims to improve the general system performance while preserving stability under normal and contingency conditions.
First step: Initially, under normal operating conditions, both HS and HHO approaches solve the OPF problem. The goals are to guarantee economic operation by means of real power losses minimization and overall fuel cost reduction, so enhancing the voltage stability over the network. All operating and security restrictions are satisfied, and generator outputs are optimized within their relevant limits. Based on optimization criteria, two algorithm performance was investigated and contrasted.
Second Step: SVC Positioning Making use of HSI combining the L-index and Vi/Vo voltage ratio index is proposed for the second phase. One can find the weakest or voltage-instability prone buses in a system by using HSI. An SVC is best found at the most vulnerable bus, based on the HSI rating, to increase voltage stability. Based on both the HS and the HHO algorithms, the OPF is re-run including the SVC; the result is compared to Step 1 to evaluate the SVC installation's effectiveness.
Third step: Contingency analysis and generator reallocation come in third. N-1 contingency analysis comes next to assess how the system responds to single transmission-line disruptions. Every contingency scenario's degree of severity was computed to identify the most catastrophic incident. Following the most severe contingency, the OPF is addressed for this defective state using generator reallocation techniques supported by both the HS and HHO to support voltage profiles and minimize system losses.
Fourth step: Re-optimizing under contingency circumstances with SVC placement comes in step four. Finally, the HIS helps one to identify the bus most affected by the selected contingency. This bus features an SVC to stop voltage instability during fault conditions. Under the contingency scenario, the OPF is run once more including SVC and generator reallocations. The total improvement in system performance was gauged by comparing the obtained results with those of past studies. This stage underlines the relative efficiency of the HS and HHO algorithms and demonstrates the usefulness of the proposed approach in handling severe system conditions.

5. RESULTS AND DISCUSSION

5.1 OPF for Normal Condition
Using an IEEE 30-bus system depicted in Figure.1 that which shows the usual line diagram of the system. The proposed approach was implemented. We investigated methodically several weight combinations of the multi-objective function, targeted at the real power generating cost, power losses, and voltage variation. Noted down and shown in Table.2 are the resultant objective function values of every weight set. From among these, the weight set W1 = 0.15, W2 = 0.10, and W3 = 0.75 resulted in the smallest objective function value and so was chosen to research further. The SVC role under Optimal Power Flow (OPF) conditions is also investigated in this work. The results demonstrate that adding SVC greatly increases voltage stability and profiles of bus performance. Four cases HHO-OPF without SVC, HS-OPF without SVC, HHO-OPF with SVC, and HS-OPF with SVC are compared in Table.3 using a relative analysis. For lowering the multi-objective function in all circumstances, the HHO method proved better than the HS method. Furthermore, enhancing generator performance, reduces power losses, and maximizes system efficiency is the presence of SVC.

Table.2: Non-Dominated Solutions for Fuel Cost, Voltage Deviation, and Transmission Losses.

Set	W_1 (FC)	W_2 (VD)	W_3 (TL)	F Value
1	0.15	0.1	0.75	210.76
2	0.22	0.1	0.68	300.09

3	0.26	0.09	0.65	349.84
4	0.295	0.105	0.6	399.93
5	0.33	0.09	0.58	449.67
6	0.385	0.08	0.535	500.02

Table.3 presents the weak bus ranking of the IEEE 30-bus system computed with the HS technique using the HSI. The Lj-index with the voltage variation index (1−Vi/V0) produces the HSI, a broad assessment of the voltage stability. With a highest value of HSI at 0.1047, the result ranks bus 30 as the least stable bus; closely followed by buses 26 and 29, both of which have major instability. Key buses are Buses 26 and 29; in order to stabilize, for example, SVC, may need reactive power supply. Conversely, buses 3, 4, and 6 were found to be most steady since their HSI values were lowest. The implementation of corrective actions, including the optimal location of reactive power compensation equipment, depends on the detection of such weak buses, hence improving system stability during Optimal Power Flow (OPF) operation.

Table.3: Weak Bus Ranking in the IEEE 30-Bus System Based on HSI Using the HS Algorithm

Rank	Bus No	Lj Value	(1 - Vi/V0) Value	HSI Value	Rank	Bus No	Lj Value	(1 - Vi/V0) Value	HSI Value
1	30	0.0891	0.1203	0.1047	13	27	0.0468	0.0849	0.06585
2	26	0.0855	0.1169	0.1012	14	22	0.0474	0.0839	0.06565
3	29	0.0732	0.1073	0.09025	15	16	0.0449	0.0791	0.062
4	24	0.0665	0.1003	0.0834	16	17	0.0439	0.08	0.06195
5	19	0.0642	0.0971	0.08065	17	9	0.0807	0.036	0.05835
6	18	0.0633	0.0958	0.07955	18	10	0.0369	0.0718	0.05435
7	25	0.0614	0.0969	0.07915	19	12	0.0374	0.0701	0.05375
8	23	0.0576	0.092	0.0748	20	7	0.0336	0.0708	0.0522
9	20	0.0575	0.0917	0.0746	21	28	0.01	0.0522	0.0311
10	21	0.0562	0.091	0.0736	22	6	0.0055	0.0446	0.02505
11	15	0.0548	0.0874	0.0711	23	4	0.0142	0.0292	0.0217
12	14	0.0523	0.0845	0.0684	24	3	0.0164	0.0122	0.0143

Likewise, Table.4 shows the weak bus ranking of the IEEE 30-bus system based on the HSI computed by the Harris Hawks Optimization (HHO) method. Based on the HSI values determined from the identical mix of the Lj-index and voltage deviation index, Bus 30 with an HSI value of 0.09785 is still the weakest bus; Bus 26 and Bus 29 follow from the results based on the HS method. These most vulnerable buses might be supported by extra reactive power or FACTS devices—that is, SVCs. On the other hand, with lowest values for HSI, buses 3, 4, and 6 were judged to be the most steady. Comparing the HS and HHO algorithm rankings confirms the effectiveness of the stability index method; the latter offers a better identification of the important buses. Achieving ideal OPF performance and improving the system resilience depend on this disparity.

The results presented in Table.5 reveal the impact of the SVC on the optimized generator outputs and total generation under both the HS and HHO methods. When comparing the scenarios with and without SVC, it is observed that the total generation is reduced in both methods when SVC is introduced. Specifically, the total generation in the HS method decreased from 299.4785 MW (without SVC) to 288.5542 MW (with SVC), whereas in the HHO method, the total generation decreased from 293.0275 MW (without SVC) to 284.8349 MW (with SVC). This reduction is expected because the SVC helps to improve the voltage profile and reduce the reactive power demand, thus lowering the need for active power generation.

The results also highlight differences in the generator outputs, with certain generators, such as PG1 and PG8, showing noticeable variations between the cases with and without SVC. Furthermore, the SVC rating remained similar in both methods, indicating that its impact on the system was consistent, regardless of the optimization technique used. These findings emphasize the effectiveness of SVC in enhancing the system stability and reducing the generation requirements while maintaining the power flow and voltage levels within acceptable limits.

Table.6 compares the important power parameters for both the HS and HHO methods with and without the SVC. The results showed clear improvements when the SVC was added to the system. For both optimization methods, the total real power generation decreased when SVC was included. The real power decreased from 299.4785 MW (without SVC) to 288.5542 MW for HS and from 293.0275 MW

to 284.8349 MW for HHO. This is expected because the SVC helps reduce the need for reactive power, which in turn lowers the overall real power demand.

Harris Hawks Optimization algorithm:

Input:

- Maximum number of iterations i_{max}
- Number of candidates N_h
- Initial random candidates or hawks C_{Nh} within specified limits (lb, ub)

Output:

- Current best solution C_{prey}

Procedure:

1. Initial random candidates or hawks C_{Nh} within specified limits (lb, ub)
2. Calculate the strength values of candidates or Hawks
3. Set C_{prey} as the best locality for the animal
4. Initialize $i = 1$
5. While (the termination condition is not satisfied) do

- For each candidate or hawk C_{Nh} , do
- Update initial energy E_o and leap strength of the animal L using:

$$E_o = 2.\,\text{rand}() - 1$$
$$L = 2(1 - \text{rand}())$$

- UpdateE using:

$$E = 2.\,E_o\left(1 - \frac{i}{i_{max}}\right)$$

- If $|E| \geq 1$, then (Exploration)

Update candidate's position by: $\text{Position} = \text{Position} + E.\,\text{rand}().\,(\text{Prey Position} - \text{Current Position})$

- Else if $E < 1$, then (Exploration)
- If $\text{rand}() \geq 0.5$ and $|E| \geq 0.5$ then (Soft Besiege)

Update candidate's position by: $\text{Position} = \text{Position} + E.\,\text{rand}().\,(\text{Prey Position} - \text{Current Position})$

- Else if $\text{rand}() < 0.5$ and $|E| < 0.5$ then (Hard Besiege)

Update candidate's position by: $\text{Position} = \text{Position} + E.\,\text{rand}().\,(\text{Prey Position} - \text{Current Position})$

- Else if $\text{rand}() < 0.5$ and $|E| \geq 0.5$, then (Soft Besiege with Quick Progressive Dives)

Update candidate's position by: $\text{Position} = \text{Position} + E.\,\text{rand}().\,(\text{prey position} - \text{current position})$

- Else if $\text{rand}() < 0.5$ and $|E| < 0.5$, then (Hard Besiege with Quick Progressive Dives)

Update candidate's position by: $\text{Position} = \text{Position} + E.\,\text{rand}().\,(\text{Prey Position} - \text{Current Position})$

- End if
- End if
- End For
- Calculate the fitness values of each candidates Hawks
- Increment I by 1
- End while

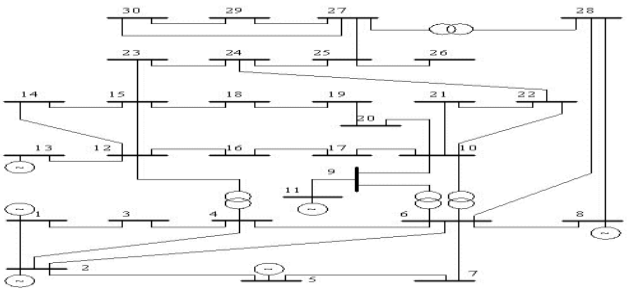

Figure.1: IEEE 30 Bus system Line Diagram

Table.4: Weak Bus Ranking in the IEEE 30-Bus System Based on HSI Using the HHO Algorithm

Rank	Bus No	Lj Value	(1 - Vi/V0) Value	HSI Value	Rank	Bus No	Lj Value	(1 - Vi/V0) Value	HSI Value
1	30	0.0825	0.1132	0.09785	13	27	0.0421	0.0797	0.0609
2	26	0.0793	0.1105	0.0949	14	22	0.0428	0.0788	0.0608
3	29	0.0678	0.1017	0.08475	15	16	0.0405	0.0742	0.05735
4	24	0.0619	0.0942	0.07805	16	17	0.0396	0.075	0.0573
5	19	0.0595	0.0918	0.07565	17	9	0.0721	0.033	0.05255
6	18	0.0584	0.0902	0.0743	18	10	0.0334	0.0674	0.0504
7	25	0.0571	0.0909	0.074	19	12	0.0339	0.0659	0.0499
8	23	0.0529	0.0864	0.06965	20	7	0.0301	0.0665	0.0483
9	20	0.0526	0.086	0.0693	21	28	0.0085	0.0481	0.0283
10	21	0.0513	0.0852	0.06825	22	6	0.0044	0.0412	0.0228
11	15	0.0497	0.0823	0.066	23	4	0.0118	0.0274	0.0196
12	14	0.0472	0.0793	0.06325	24	3	0.0135	0.0105	0.012

Table.5: Optimized Generator Outputs and Total Generation for HS and HHO Methods With and Without SVC

Method	PG1 (MW)	PG2 (MW)	PG5 (MW)	PG8 (MW)	PG11 (MW)	PG13 (MW)	Total Generation (MW)	SVC Rating
HS without SVC	137.4123	33.3926	30.0535	43.7988	44.8213	10	299.4785	---------
HS with SVC	122.7512	32.3868	29.1793	42.4472	41.7897	10	288.5542	0.06789
HHO without SVC	132.1714	15.3346	24.7193	21.9864	78.8158	10	293.0275	---------
HHO with SVC	127.9793	15.0957	25.3001	20.3371	76.1227	10	284.8349	0.06787

Table.6: Power Parameters Comparison of HS and HHO Methods With and Without SVC

Parameter	HS without SVC	HS with SVC	HHO without SVC	HHO with SVC
Total Real Power (MW)	299.4785	288.5542	293.0275	284.8349
Real Power Loss (MW)	16.0785	5.1542	9.6275	1.4349
Reactive Power Loss (MVAR)	33.35	13.55	17.38	10.97
Voltage Deviation (p.u.)	2.444	0.2338	1.8947	0.2293
Fuel Cost ($/hr)	1361.9	1278.5	1355.7	1262.2

In terms of power losses, both the real and reactive power losses were significantly reduced with SVC. For example, the real power loss decreased from 16.0785 MW to 5.1542 MW for HS and from 9.6275 MW to 1.4349 MW for HHO. Similarly, reactive power loss drops from 33.35 MVAR to 13.55 MVAR for HS, and from 17.38 MVAR to 10.97 MVAR for HHO. These results highlight the effectiveness of SVC in improving the efficiency of the system by reducing both types of power loss. Additionally, the fuel cost for generating power is lower when SVC is used, indicating better cost efficiency. The fuel cost decreases from $1361.9 per hour to $1278.5 per hour for HS and from $1355.7 per hour to $1262.2 per hour for HHO. This shows that the generation process was more optimized with reduced losses.

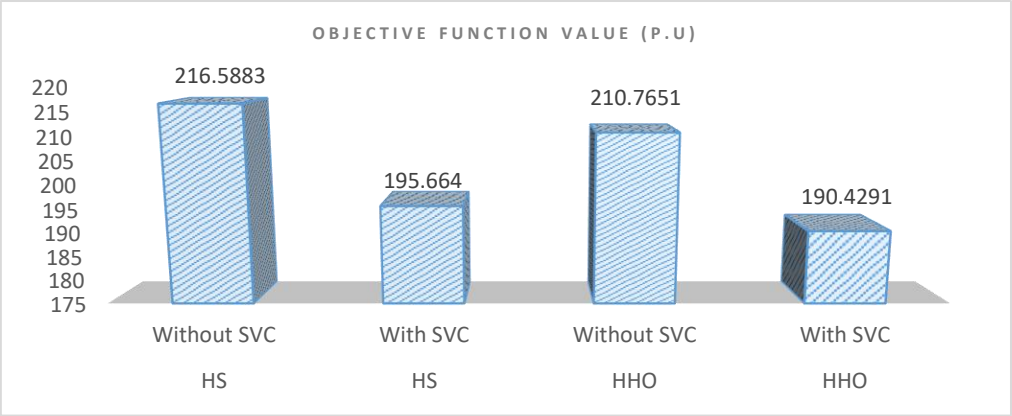

Figure.2: Objective Function (F) Comparison for HS and HHO Algorithms with and Without SVC

Figure.2 compares the HS and HHO algorithms in two scenarios: with and without a SVC. The results showed significant improvements when SVC was used. First, the fuel cost decreases when the SVC is applied. For the HS, the cost drops from $1361.9 per hour without SVC to $1278.5 per hour with SVC. For HHO, it falls from $1355.7 per hour to $1262.2 per hour. This shows that SVC helps reduce the generator costs. Next, the voltage stability improves with SVC. HS shows a large reduction in voltage deviation from 2.444 p.u. to 0.2338 p.u., while HHO improves from 1.8947 p.u. to 0.2293 p.u.. This means that the system becomes more stable with SVC. The real power loss also decreased, particularly with the HHO method. The loss reduces from 9.6275 MW to only 1.4349 MW when SVC is used, making the system more efficient. Finally, the F value, which combines the fuel cost, voltage deviation, and power loss, shows that HHO with SVC performs best, with a value of 190.4291, followed by HS with SVC at 195.664.

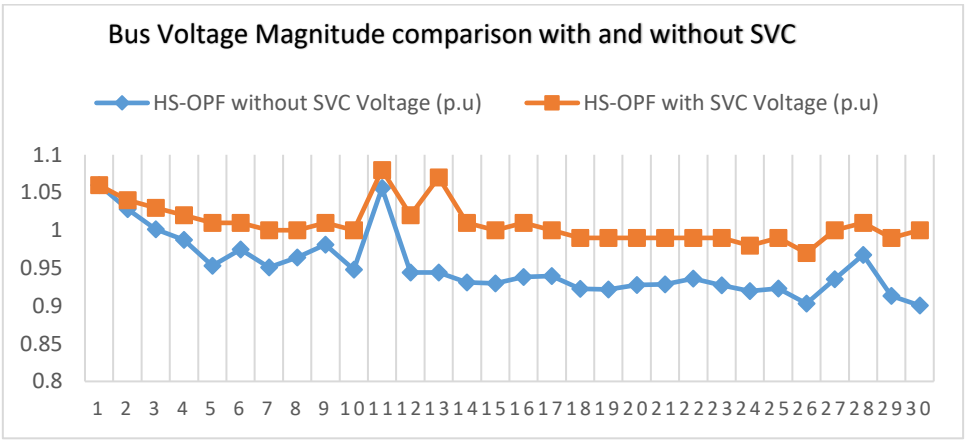

Figure.3: Bus-Wise Voltage Magnitude Comparison Using HS-OPF With and Without SVC

In Figure.3 the HS-OPF analysis of the IEEE 30-bus system and the integration of a SVC effectively enhanced the voltage profile and improved the voltage stability across the network. Without the SVC, the lowest recorded voltage magnitude was 0.90055 p.u. at Bus 30, which was significantly improved to 1.00 p.u. after including the SVC. Buses such as 13, 12, and 14 experienced major voltage magnitude improvements: Bus 13 increased from 0.94409 to 1.07 p.u., Bus 12 from 0.94418 to 1.02 p.u., and Bus 14 from 0.93095 to 1.01 p.u. Similarly, Bus 29 rose from 0.91321 to 0.99 p.u., and Bus 27 from 0.93521 to 1.00 p.u., showcasing improved reactive power support across critical load buses.

The voltage angles also shifted slightly, generally becoming more negative with the SVC, highlighting the system's response to reactive power adjustments. For instance, the angle of Bus 3 changed from -3.06° to -3.49°, that of Bus 11 from -0.26° to -1.10°, and that of Bus 30 from -11.45° to -11.81°. While the magnitude of the angles slightly increased in negativity, the uniformity in the angles suggests better power flow balancing. Overall, the HS-OPF with SVC maintained higher voltage levels and a more balanced voltage angle distribution, indicating improved operational conditions and better voltage regulation throughout the system.

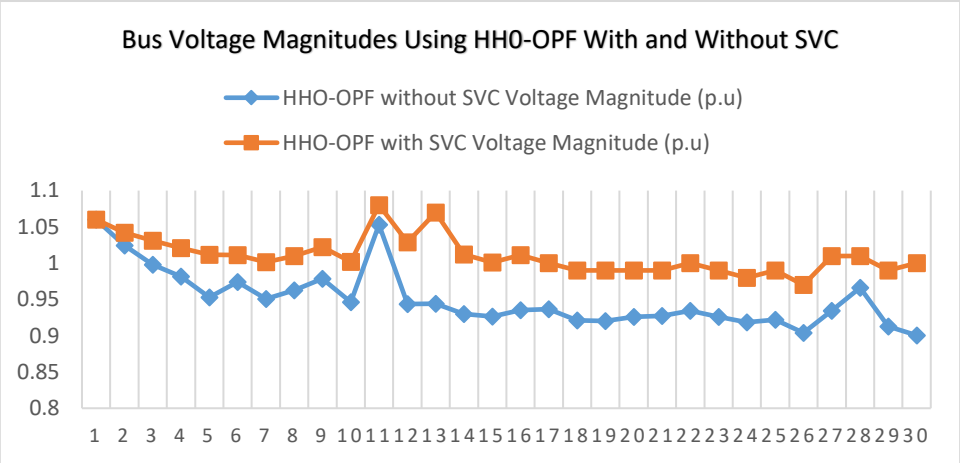

Figure.4: Bus-Wise Voltage Magnitude Comparison Using HHO-OPF With and Without SVC

In Figure.4 the HHO-OPF analysis performed on the 30-bus system, the incorporation of a SVC resulted in notable improvements in both voltage magnitudes and voltage angles across most buses. Without SVC, voltage magnitudes dropped as low as 0.90055 p.u. (Bus 30), while with SVC, the minimum voltage magnitude was improved to 1.00 p.u., indicating enhanced voltage stability. Significant voltage magnitude improvements were observed at Bus 13 (from 0.94409 to 1.07 p.u.), Bus 12 (from 0.94384 to 1.029 p.u.), and Bus 14 (from 0.92983 to 1.012 p.u.). Similarly, buses such as 29 and 30 saw substantial voltage gains, with Bus 29 increasing from 0.91282 to 0.99 p.u., and Bus 30 from 0.90055 to 1.00 p.u.

In terms of voltage angles, the maximum negative angle without SVC was observed at Bus 30 with -11.5013°, whereas with SVC, it became slightly more negative at -11.8617°. However, across many buses, the SVC helped in reducing angle deviations. For instance, Bus 2's angle changed from -1.81021° to -2.20145°, and Bus 3's from -3.09745° to -3.54238°, reflecting the reactive power support balancing effects of SVC. In contrast, several buses saw minimal changes in angles, indicating that the main impact of SVC was more pronounced on voltage magnitudes. Overall, the inclusion of SVC in the HHO-OPF framework significantly improved voltage profile uniformity and system voltage stability across the entire 30-bus network.

5.2 OPF for Contingency Condition

Table.7 presents the contingency severity ranking for the IEEE 30-bus system using the HSI based on the HS optimization method. The contingency analysis is conducted under N-1 conditions, assuming that a single transmission line fails at a time. The results reveal that the outage of the transmission line connecting Buses 27 and 28 places the highest stress on the power system, with a peak HSI value of 0.3832 p.u., indicating a severe deterioration in voltage stability and an increased risk of operational imbalance. This makes Line 27–28 the most critical single-line contingency.

The table provides a detailed breakdown of the contingency analysis, showing the Lj value (line loading severity), the (1 - Vi/V0) value (relative voltage drop at the weakest bus), the bus number with the highest HSI value, and the corresponding HSI value for each line outage. In multiple contingencies, Bus 30 consistently emerges as the most affected node, highlighting its vulnerability to disturbances. To mitigate this vulnerability and improve the system's resilience, further analysis suggests deploying a SVC at Bus 30. The SVC aims to enhance voltage stability and provide reactive power compensation during worst-case outage scenarios.

In addition to Line 27–28, other high-risk lines, such as Line 14 (Bus 9–10) and Line 38 (Bus 27–30), also show elevated HSI values, although to a lesser extent. These results underscore the importance of strategically deploying FACTS devices, like SVCs, in regions vulnerable to voltage instability. Overall, the study highlights the role of such devices in strengthening the power system's security, particularly during critical disturbances that may lead to voltage instability.

Table.8 presents the contingency severity ranking for the IEEE 30-bus system using the HSI based on the HHO method. The analysis is conducted under N-1 conditions, assuming the failure of a single transmission line at a time. The results indicate that the outage of the transmission line between Buses 27 and 28 causes the most significant stress on the system, with an HSI value of 0.3884 p.u. This high value reflects a severe deterioration in voltage stability and indicates the criticality of Line 27–28 in maintaining system stability. The table provides a breakdown of the contingency analysis for each line

outage, including the Lj value (line loading severity), the (1 - Vi/V0) value (which measures the relative voltage drop at the weakest bus), the bus with the highest HSI value, and the HSI value. The results highlight that Bus 30 consistently exhibits the highest HSI value, signalling its vulnerability under various contingencies. Following the outage of Line 27–28, other significant lines include Line 14 (Bus 9–10) and Line 38 (Bus 27–30), though their impact is less severe compared to Line 27–28. As in previous analyses, Bus 30 remains the most vulnerable bus, emphasizing the need for mitigation strategies to strengthen its resilience. To enhance system stability, a SVC at Bus 30 is recommended to improve voltage stability and provide reactive power support during critical contingencies. The results underscore the importance of strategic deployment of FACTS devices, such as SVCs, to improve voltage regulation and system reliability during contingency events.

Table.7: HSI-Based Contingency Severity Ranking using HS based OP for the IEEE 30-bus system.

Line No	From Bus to Bus	Lj Value	(1 - Vi/V0) Value	Bus No (HSI max)	HSI	Line No	From Bus to Bus	Lj Value	(1 - Vi/V0) Value	Bus No (HSI max)	HSI
36	27 to 28	0.438	0.3285	30	0.3832	28	10 to 22	0.095	0.1227	26	0.1131
14	9 to 10	0.182	0.1937	19	0.1879	31	22 to 24	0.095	0.1227	26	0.1131
38	27 to 30	0.168	0.177	30	0.1724	3	2 to 4	0.087	0.1301	30	0.1131
5	2 to 5	0.111	0.2378	30	0.1691	18	12 to 15	0.087	0.1198	30	0.1091
15	4 to 12	0.151	0.1821	15	0.1662	12	6 to 10	0.086	0.1173	30	0.1082
37	27 to 29	0.154	0.165	29	0.1594	32	23 to 24	0.085	0.1171	30	0.1078
2	1 to 3	0.106	0.2084	30	0.1592	29	21 to 23	0.084	0.1156	30	0.1065
4	3 to 4	0.108	0.2051	30	0.1569	8	5 to 7	0.083	0.1149	30	0.1061
27	10 to 21	0.131	0.1523	21	0.1442	17	12 to 14	0.083	0.1147	30	0.1059
35	25 to 27	0.129	0.1504	26	0.1426	19	12 to 16	0.083	0.1146	30	0.1058
41	6 to 28	0.122	0.1507	30	0.1413	22	15 to 18	0.082	0.1143	30	0.1057
25	10 to 20	0.127	0.1446	20	0.1393	30	15 to 23	0.082	0.114	30	0.1056
6	2 to 6	0.098	0.1724	30	0.1388	23	18 to 19	0.082	0.1138	30	0.1055
7	4 to 6	0.099	0.1605	30	0.1345	20	14 to 15	0.082	0.1137	30	0.1055
39	29 to 30	0.106	0.1364	30	0.1277	40	8 to 28	0.082	0.1136	30	0.1054
24	19 to 20	0.109	0.1317	19	0.1252	21	16 to 17	0.082	0.1135	30	0.1053
10	6 to 8	0.121	0.1342	30	0.1245	11	6 to 9	0.078	0.1104	30	0.1023
26	10 to 17	0.108	0.1286	17	0.1218	33	24 to 25	0.075	0.1078	30	0.0994

Table.8: HSI-Based Contingency Severity Ranking using HHO based OP for the IEEE 30-bus system

Line No	From Bus to Bus	Lj Value	(1 - Vi/V0) Value	Bus No (HSI max)	HSI	Line No	From Bus to Bus	Lj Value	(1 - Vi/V0) Value	Bus No (HSI max)	HSI
36	27 to 28	0.432	0.3448	30	0.3884	28	10 to 22	0.099	0.1274	26	0.1132
14	9 to 10	0.182	0.2051	19	0.1936	31	22 to 24	0.098	0.1271	26	0.1126
38	27 to 30	0.174	0.1843	30	0.1792	3	2 to 4	0.089	0.1346	30	0.1118
5	2 to 5	0.117	0.2438	30	0.1665	18	12 to 15	0.088	0.1245	30	0.1063
15	4 to 12	0.153	0.1867	15	0.1699	12	6 to 10	0.087	0.1213	30	0.1042
37	27 to 29	0.156	0.1715	29	0.1637	32	23 to 24	0.087	0.121	30	0.104
2	1 to 3	0.111	0.2143	30	0.1626	29	21 to 23	0.086	0.1192	30	0.1027
4	3 to 4	0.108	0.2108	30	0.1594	8	5 to 7	0.084	0.12	30	0.102
27	10 to 21	0.137	0.1582	21	0.1476	17	12 to 14	0.083	0.1191	30	0.1011
35	25 to 27	0.133	0.1534	26	0.1432	19	12 to 16	0.083	0.119	30	0.101
41	6 to 28	0.125	0.1541	30	0.1395	22	15 to 18	0.083	0.1187	30	0.1008
25	10 to 20	0.128	0.1495	20	0.1388	30	15 to 23	0.082	0.1183	30	0.1002
6	2 to 6	0.099	0.1754	30	0.1372	23	18 to 19	0.08	0.113	30	0.105
7	4 to 6	0.098	0.1623	30	0.1302	20	14 to 15	0.08	0.113	30	0.105
39	29 to 30	0.11	0.1374	30	0.1237	40	8 to 28	0.08	0.113	30	0.105
24	19 to 20	0.111	0.1342	19	0.1226	21	16 to 17	0.08	0.113	30	0.105
10	6 to 8	0.121	0.1379	30	0.125	11	6 to 9	0.07	0.110	30	0.102
26	10 to 17	0.112	0.1327	17	0.1223	33	24 to 25	0.07	0.107	30	0.099

Table.9: Generation Optimization during Line Outage (Bus 27–28) with SVC Support

Method	PG1 (MW)	PG2 (MW)	PG5 (MW)	PG8 (MW)	PG11 (MW)	PG13 (MW)	Total Generation (MW)	SVC Rating
HS without SVC	138.7838	33.6619	30.2649	44.0519	35.5029	10	302.2654	---------

HS with SVC	128.4529	33.0742	29.7416	43.3309	37.4528	10	292.0524	0.1529
HHO without SVC	134.0653	15.4302	24.8722	22.0955	78.7936	10	295.2568	---------
HHO with SVC	130.7128	15.1834	25.4158	20.4512	75.1646	10	286.9268	0.1527

Table.9 presents the results of generation optimization during the outage of the transmission line between Bus 27 and Bus 28, comparing the system performance with and without the support of a SVC. In the scenario without SVC, the total generation using the HS method is 302.2654 MW, while the HHO method results in a total generation of 295.2568 MW. When SVC support is introduced, the total generation decreases slightly for both methods, with HS showing a total generation of 292.0524 MW and HHO showing 286.9268 MW. The SVC rating is 0.1529 for HS and 0.1527 for HHO, indicating the compensatory role of the SVC in providing reactive power support during the outage. These results highlight the effectiveness of SVC in improving system stability and reducing the total generation required by redistributing power across the generators, enhancing the system's overall efficiency.

Table.10 compares the total power generation, losses, and fuel costs during the line outage between Bus 27 and Bus 28, both with and without the support of a SVC for the HS and HHO methods. During the line outage, without SVC, the total real power generated is 302.2654 MW for HS and 295.2568 MW for HHO. When SVC is applied, the total generation decreases slightly to 292.0524 MW for HS and 286.9268 MW for HHO, demonstrating that the SVC helps reduce the generation requirement by improving system stability and mitigating the impact of the outage. Real power losses are significantly reduced with SVC. Without SVC, the real power loss during the line outage is 18.8654 MW for HS and 11.8568 MW for HHO. With SVC, the losses decrease to 8.6524 MW for HS and 3.5268 MW for HHO, showing that SVC effectively minimizes the power loss caused by the line outage. Similarly, reactive power losses are reduced when SVC is applied. Without SVC, reactive power losses are 35.7 MVAR for HS and 19.27 MVAR for HHO, while with SVC, they drop to 18.73 MVAR for HS and 12.31 MVAR for HHO, further emphasizing the role of SVC in improving the stability and efficiency of the system during the outage. Finally, fuel costs also decrease with the use of SVC. The fuel cost for HS without SVC during the line outage is $1375.7/hr, which reduces to $1287.3/hr with SVC. For HHO, the fuel cost without SVC is $1383.2/hr, and with SVC, it reduces to $1264.5/hr. This reduction in fuel costs indicates that the addition of SVC not only improves the overall efficiency of the power system during the outage but also reduces operational costs.

Table.10: Total Power Generation and Losses

Parameter	HS without SVC	HS with SVC	HHO without SVC	HHO with SVC
Total Real Power (MW)	302.2654	292.0524	295.2568	286.9268
Real Power Loss (MW)	18.8654	8.6524	11.8568	3.5268
Reactive Power Loss (MVAR)	35.7	18.73	19.27	12.31
Voltage Deviation (p.u.)	4.782	2.2338	2.8947	1.2293
Fuel Cost ($/hr)	1375.7	1287.3	1383.2	1264.5

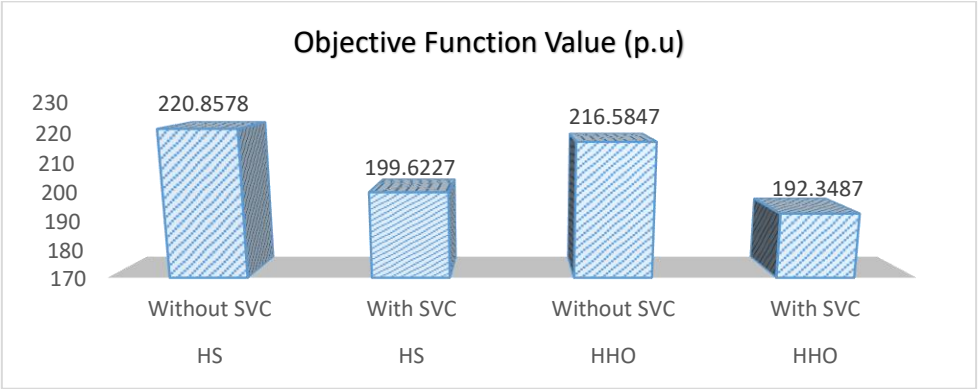

Figure.5: Objective Function (F) Comparison for HS and HHO Algorithms with and Without SVC

In Figure.5 The results clearly show that the inclusion of a SVC improves the F1 performance metric for both optimization algorithms. For the HS algorithm, the F1 value reduces significantly from 220.8578 (without SVC) to 199.6227 (with SVC). Similarly, the HHO algorithm exhibits an F1 value

reduction from 216.5847 (without SVC) to 192.3487 (with SVC). This consistent decrease in F1 value with SVC inclusion indicates better optimization performance, as lower F1 values typically correspond to improved cost, power loss, and voltage deviation metrics in multi-objective OPF formulations. Among all scenarios, the HHO with SVC case yields the lowest F1 value (192.3487), establishing it as the most effective configuration in terms of overall objective function performance.

Table.11 shows the bus voltage magnitudes in both pre-contingency and post-contingency states for the HS algorithm-based Optimal Power Flow (OPF) with and without SVC support during the line outage (Bus 27–28).In the pre-contingency state, the voltage magnitudes at all buses remain relatively stable, with minor variations between the scenarios with and without SVC. For example, Bus 1, which maintains a voltage magnitude of 1.06 p.u. in both cases, shows consistent results across both conditions. Similarly, Bus 2 has pre-contingency voltages of 1.02812 p.u. (without SVC) and 1.04 p.u. (with SVC), indicating only slight improvements with SVC. However, the post-contingency voltage magnitudes reveal significant improvements when SVC is applied. For instance, after the contingency, Bus 16 experiences a notable drop in voltage from 0.93834 p.u. (without SVC) to 1.01 p.u. (with SVC). Likewise, Bus 27, which has a post-contingency voltage of 0.93521 p.u. without SVC, increases to 1.01 p.u. with SVC, demonstrating the compensatory benefits of the SVC in maintaining voltage stability. Other buses such as Bus 3, Bus 4, Bus 5, and Bus 8 show similar improvements in their post-contingency voltage values, highlighting the positive role of SVC in stabilizing voltage levels during contingency events. In particular, buses closer to the outage area, like Bus 27, Bus 28, and Bus 30, see the most significant enhancements in voltage magnitude due to SVC activation, which improves their voltage stability and reduces the risk of voltage collapse. Overall, Table 11 illustrates that the implementation of SVC enhances voltage stability by reducing the magnitude of voltage drops post-contingency, thereby improving system resilience during critical events like the Bus 27–28 line outage.

Table.11: Bus voltage magnitudes in pre & post contingency state in Harmony Search algorithm based OPF without & with SVC

Bus No	Pre-Contingency Voltage (p.u.)		Post-Contingency Voltage (p.u.)		Bus No	Pre-Contingency Voltage (p.u.)		Post-Contingency Voltage (p.u.)	
	HS-based OPF without SVC	HS-based OPF with SVC	HS-based OPF without SVC	HS-based OPF with SVC		HS-based OPF without SVC	HS-based OPF with SVC	HS-based OPF without SVC	HS-based OPF with SVC
1	1.06	1.06	1.06	1.06	16	0.93834	1.01	0.8842	1.01
2	1.02812	1.04	1.0065	1.04	17	0.93935	1	0.8794	1
3	1.00123	1.03	0.9751	1.03	18	0.92247	0.99	0.8633	0.99
4	0.98731	1.02	0.9558	1.02	19	0.9218	0.99	0.8611	0.99
5	0.95289	1.01	0.9169	1.01	20	0.92758	0.99	0.8673	0.99
6	0.97485	1.01	0.9401	1.01	21	0.92863	0.99	0.861	0.99
7	0.95112	1	0.9155	1	22	0.93617	0.99	0.8565	1
8	0.96394	1	0.9284	1.01	23	0.92741	0.99	0.8574	0.99
9	0.98105	1.01	0.9321	1.02	24	0.91964	0.98	0.8141	0.98
10	0.94802	1	0.8872	1	25	0.92319	0.99	0.7342	0.99
11	1.05587	1.08	1.0139	1.08	26	0.90326	0.97	0.7091	0.97
12	0.94418	1.02	0.8991	1.03	27	0.93521	1	0.6997	1.01
13	0.94409	1.07	0.8992	1.07	28	0.96742	1.01	0.9402	1.01
14	0.93095	1.01	0.8807	1.01	29	0.91321	0.99	0.6691	0.99
15	0.92958	1	0.8736	1	30	0.90055	1	0.6509	1

Table.12: Bus voltage magnitudes in pre & post contingency state in HHO algorithm based OPF without & with SVC

Bus No	Pre-Contingency Voltage (p.u.)		Post-Contingency Voltage (p.u.)		Bus No	Pre-Contingency Voltage (p.u.)		Post-Contingency Voltage (p.u.)	
	HHO-based OPF without SVC	HHO - based OPF with SVC	HHO - based OPF without SVC	HHO - based OPF with SVC		HHO-based OPF without SVC	HHO - based OPF with SVC	HHO - based OPF without SVC	HHO - based OPF with SVC
1	1.06	1.06	1.06	1.06	16	0.93541	1.011	0.8886	1.011
2	1.02431	1.042	1.0089	1.042	17	0.93657	1	0.883	1
3	0.99792	1.031	0.9792	1.031	18	0.92103	0.99	0.8682	0.99
4	0.98156	1.021	0.9604	1.021	19	0.92027	0.99	0.8653	0.99

5	0.95289	1.0115	0.9206	1.0115	20	0.92617	0.99	0.8705	0.99
6	0.97418	1.011	0.9443	1.011	21	0.92734	0.99	0.8651	0.99
7	0.95053	1.0015	0.919	1.0015	22	0.93447	1	0.86	1
8	0.96261	1.01	0.9321	1.01	23	0.92602	0.99	0.8612	0.99
9	0.97842	1.022	0.9352	1.022	24	0.91864	0.98	0.8176	0.98
10	0.94633	1.002	0.8912	1.002	25	0.92212	0.99	0.738	0.99
11	1.05321	1.08	1.0176	1.08	26	0.90376	0.97	0.7132	0.97
12	0.94384	1.029	0.9025	1.029	27	0.93421	1.01	0.7036	1.01
13	0.94409	1.07	0.902	1.07	28	0.96637	1.01	0.943	1.01
14	0.92983	1.012	0.8849	1.012	29	0.91282	0.99	0.6729	0.99
15	0.92644	1.001	0.8782	1.001	30	0.90055	1	0.6552	1

Table.12 presents the bus voltage magnitudes in the pre-contingency and post-contingency states for the HHO (Harris Hawks Optimization) algorithm-based OPF, both with and without SVC support, during the line outage between Bus 27–28.In the pre-contingency state, the voltage magnitudes at all buses show relatively stable values in both scenarios, with slight variations between the setups with and without SVC. For instance, at Bus 1, the voltage is 1.06 p.u. in both cases, indicating no significant difference in the pre-contingency state. Similarly, Bus 2 has a voltage of 1.02431 p.u. without SVC and 1.042 p.u. with SVC, showing a minor increase with the addition of SVC. In the post-contingency state, however, there are noticeable improvements when SVC is implemented. For example, at Bus 16, the voltage drops from 0.93541 p.u. (without SVC) to 1.011 p.u. (with SVC), showing a considerable recovery due to SVC. Similar trends are observed at other buses, such as Bus 17, which improves from 0.93657 p.u. to 1 p.u., and Bus 18, which rises from 0.92103 p.u. to 0.99 p.u. when SVC is applied. Other buses also demonstrate clear voltage stabilization post-contingency with the introduction of SVC. For example, Bus 24 sees an increase in voltage from 0.91864 p.u. to 0.98 p.u., and Bus 26 improves from 0.90376 p.u. to 0.97 p.u. These results highlight the effectiveness of SVC in enhancing voltage recovery after the contingency event, especially in areas closer to the outage. Overall, Table.12 shows that the application of SVC results in improved voltage stability during contingency scenarios, with most buses experiencing a boost in post-contingency voltage magnitude. This reinforces the role of SVC in mitigating voltage instability and ensuring system resilience during outages.

6. CONCLUSION

HHO algorithm performs better than the HS algorithm in improving voltage stability, optimizing power generation, and reducing costs. HHO, especially with SVC support, offers better voltage stability during contingencies. For example, at Bus 16 and Bus 27, HHO maintains higher voltage stability after a contingency compared to HS. Additionally, HHO is more effective in minimizing real power losses and fuel costs. With SVC, HHO generated 286.9268 MW at a fuel cost of $1264.5/hr, while HS with SVC generated 292.0524 MW but at a higher cost of $1287.3/hr. Overall, the HHO algorithm is more efficient and reliable, making it the better choice for improving power system stability and cutting operational costs, especially during contingency events and when SVC is used.

References

1. Acha, E., Fuerte-Esquivel, C., Ambriz-Perez, H., Angeles, C.: FACTS: Modelling and Simulation in Power Networks, pp. 105–120. Wiley (2004). https://doi.org/10.1002/0470020164
2. Roberto Minguez; Federico Milano; Rafael Zarate-Minano; Antonio J. Conejo “Optimal Network Placement of SVC Devices” IEEE Transactions on Power Systems (Volume: 22, Issue: 4, November 2007) Page(s): 1851 – 1860 DOI: 10.1109/TPWRS.2007.907543
3. D.J. Gotham; G.T. Heydt “Power flow control and power flow studies for systems with FACTS devices” IEEE Transactions on Power Systems (Volume: 13, Issue: 1, February 1998) Page(s): 60 – 65 DOI: 10.1109/59.651614
4. Canbing Li; Liwu Xiao; Yijia Cao; Qianlong Zhu; Baling Fang; Yi Tan “ Optimal allocation of multi-type FACTS devices in power systems based on power flow entropy ” Journal of Modern Power Systems and Clean Energy (Volume: 2, Issue: 2, June 2014) Page(s): 173 – 180 DOI: 10.1007/s40565-014-0059-x
5. Kothari, D., & Nagrath, I., "Modern power system analysis," Tata McGraw Hill Education Private Limited, 2017.
6. Mahrous El-Azab; Walid A. Omran; Said Fouad Mekhamer; Hossam E. A. Talaat “Allocation of FACTS Devices Using a Probabilistic Multi-Objective Approach Incorporating Various Sources of Uncertainty and Dynamic Line Rating” IEEE Access (Volume: 8) Page(s): 167647 – 167664 DOI: 10.1109/ACCESS.2020.3023744
7. Shraddha Udgir; Laxmi Srivastava; Manjaree Pandit “Optimal placement and sizing of SVC for loss minimization and voltage security improvement using differential evolution algorithm” International Conference on Recent Advances

and Innovations in Engineering (ICRAIE-2014) Date of Conference: 09-11 May 2014 DOI: 10.1109/ICRAIE.2014.6909310

8. Hossam S. Salama , István Vokony "Voltage stability indices–A comparison and a review" Computers & Electrical Engineering Volume 98, March 2022, 10774 doi.org/10.1016/j.compeleceng.2022.107743
9. Javad Modarresi, Eskandar Gholipour, Amin Khodabakhshian "A comprehensive review of the voltage stability indices" Renewable and Sustainable Energy Reviews Volume 63, September 2016, Pages 1-12 doi.org/10.1016/j.rser.2016.05.010
10. Saurabh Ratra, Rajive Tiwari, K.R. Niazi "Voltage stability assessment in power systems using line voltage stability index" Computers & Electrical Engineering Volume 70, August 2018, Pages 199-211 doi.org/10.1016/j.compeleceng.2017.12.046
11. Ch. Jayasree , B. Sravan Kumar " Krill Herd Algorithm Based Real Power Generation Reallocation for Improvement of Voltage Profile" Procedia Computer Science Volume 92, 2016, Pages 36-41 doi.org/10.1016/j.procs.2016.07.320
12. B. Venkateswara Rao, G.V. Nagesh Kumar "Optimal power flow by BAT search algorithm for generation reallocation with unified power flow controller" International Journal of Electrical Power & Energy Systems Volume 68, June 2015, Pages 81-88 doi.org/10.1016/j.ijepes.2014.12.057
13. B. Muruganantham , R. Gnanadass, N.P. Padhy "Reactive Power Reallocation in the Distribution System with DSTATCOM" Energy Procedia Volume 117, June 2017, Pages 485-492 doi.org/10.1016/j.egypro.2017.05.174
14. G. V. Nagesh Kumar, B. Sravana Kumar, B. Venkateswara Rao & D. Deepak Chowdary "Enhancement of Voltage Stability Using FACTS Devices in Electrical Transmission System with Optimal Rescheduling of Generators by Brain Storm Optimization Algorithm" ©Springer Nature Switzerland AG 2019 S. Cheng and Y. Shi (eds.), Brain Storm Optimization Algorithms, Adaptation, Learning, and Optimization 23, https://doi.org/10.1007/978-3-030-15070-9_11
15. Asaju La'aro Bolaji , Mohammed Azmi Al-Betar , Mohammed A. Awadallah , Ahamad Tajudin Khader , Laith Mohammad Abualigah "A comprehensive review: Krill Herd algorithm (KH) and its applications" Applied Soft Computing Volume 49, December 2016, Pages 437-446 doi.org/10.1016/j.asoc.2016.08.041
16. Nampetch Sinsuphan, Uthen Leeton, Thanatchai Kulworawanichpong "Optimal power flow solution using improved harmony search method" Applied Soft Computing Volume 13, Issue 5, May 2013, Pages 2364-2374 doi.org/10.1016/j.asoc.2013.01.024
17. M.A. Abido "Optimal power flow using particle swarm optimization" International Journal of Electrical Power & Energy Systems Volume 24, Issue 7, October 2002, Pages 563-571 doi.org/10.1016/S0142-0615(01)00067-9
18. Mohammad Zohrul Islam; Noor Izzri Abdul Wahab; Veerapandiyan Veerasamy; Hashim Hizam; Nashiren Farzilah Mailah; Abdullah Khan "Optimal Power Flow using a Novel Harris Hawk Optimization Algorithm to Minimize Fuel Cost and Power loss" 2019 IEEE Conference on Sustainable Utilization and Development in Engineering and Technologies (CSUDET) Date of Conference: 07-09 November 2019 10.1109/CSUDET47057.2019.9214591
19. A. G. Bakirtzis, P. N. Biskas, C. E. Zoumas, and V. Petridis, "Optimal power flow by enhanced genetic algorithm," IEEE Trans. Power Syst., vol. 17, no. 2, pp. 229–236, May 2002. 10.1109/TPWRS.2002.1007886
20. H.W.Dommel and W.Tinney, "Optimal power flow solutions," IEEE Trans. Power Appar. Syst.,vol.pas-87,no.10,pp.1866–1876,1968. 29 January 2007 , 10.1109/TPAS.1968.292150
21. M. A. Abido, "Optimal power flow using tabu search algorithm," Electr. Power Components Syst., vol. 30, no. 5, pp. 469–483, May 2002. doi.org/10.1080/15325000252888425
22. A. A. Abou El Ela, M. A. Abido, and S. R. Spea, "Optimal power flow using differential evolution algorithm," Electr. Power Syst. Res., vol. 80, no. 7, pp. 878–885, Jul. 2010. doi.org/10.1016/j.epsr.2009.12.018
23. T. N. Le Anh, D. N. Vo, W. Ongsakul, P. Vasant, and T. Ganesan, "Cuckoo optimization algorithm for optimal power flow," 2015, pp. 479–493. Cuckoo Optimization Algorithm for Optimal Power Flow | SpringerLink
24. A. Mishra, V. N. K. Gundavarapu, Contingency management of power system with Interline Power Flow Controller using Real Power Performance Index and Line Stability Index, Ain Shams Engineering Journal 7(1)(2016) 209-222. doi.org/10.1016/j.asej.2015.11.004
25. AmirH.Gandomia & AmirH.Alavib. An introduction of Krill Herd algorithm for engineering optimization, Journal of Civil Engineering and Management 22(3)(2016) 302-310. https://doi.org/10.3846/13923730.2014.897986
26. J. Preetha Roselyn, D. Devaraj, Subhransu Sekhar Dash, Multi Objective Genetic Algorithm for voltage stability enhancement using rescheduling and FACTS devices, Ain shams Engineering Journal 5 (2014) 789-801. doi.org/10.1016/j.asej.2014.04.004
27. F.KhandaniI,S.SoleymaniI,B.Mozafari, Optimal Placement of SVC to Improve Voltage Profile Using Hybrid Genetics Algorithm and Sequential Quadratic Programming, Electrical Power Distribution Networks (EPDC), 16th Conference on 19-20 April (2011) 1- 6 Optimal placement of SVC to improve voltage profile using hybrid genetics algorithm and Sequential Quadratic Programming | IEEE Conference Publication | IEEE Xplore
28. P. Jirapong & W. Ongsakul. Optimal Placement of Multi-Type FACTS Devices for Total Transfer Capability Enhancement Using Hybrid Evolutionary Algorithm, Electric Power Components and Systems 35(9)(2007)981–1005. https://doi.org/10.1080/15325000701249993
29. A. R. Phadke, Manoj Fozdar, and K. R. Niazi. A New Multi objective Formulation for Optimal Placement of Shunt Flexi ble AC Transmission Systems Controller. Electric Power Components and Systems 37(12)(2009) 1386–1402. https://doi.org/10.1080/15325000903055305
30. T. P. Nam, D. T. Viet La Van Ut., Optimal Placement of SVC in Power Market, IEEE 9th Conference on Industrial Electronics and Applications (ICIEA), Hangzhou, China, June 9-11, (2014)1713 1718. 10.1109/ICIEA.2014.6931444